Characterization of Gas–Liquid Two-Phase Flow by Correlation Dimension of Vortex-Induced Pressure Fluctuation

SISHI HUANG, JIAWEN YIN, ZHIQIANG SUN, SAIWEI LI, AND TIAN ZHOU
School of Energy Science and Engineering, Central South University, Changsha 410083, China
Corresponding author: Zhiqiang Sun (zqsun@csu.edu.cn)

ABSTRACT Characterization of flow behaviors is one of the most challenging problems in a gas–liquid flow system. In this paper, correlation dimension, a chaotic characteristic indicator, was introduced to characterize the gas–liquid two-phase flow behaviors by using the fluctuating pressure induced by a bluff body. An artificial neural network was trained to help select suitable flow parameters that were combined with correlation dimension to construct a novel gas–liquid flow pattern map, which was able to distinguish between the bubble, bubble/plug transitional, plug, slug, and annular flows with reasonable accuracy. Furthermore, a quantitative correlation with the form of $u_{\mathrm{g}} = AD_2^B u^C$ was established by the universal fitting and the pattern-specific fitting with the coefficients of determination R^2 approaching to 1. In view of the simplicity and the convenience of vortex generation and pressure measurement, the correlation dimension-based method provides an effective and practical idea to gas–liquid two-phase flows study.

INDEX TERMS Gas–liquid flow, correlation dimension, flow characterization, vortex-induced pressure fluctuation, artificial neural network.

I. INTRODUCTION

Gas–liquid two-phase flow abounds in various industrial equipment and processes [1]. Characterization of its flow behaviors is known as one of the biggest challenges in the field of multiphase flow study, due to the highly deformable interfaces between the gaseous and liquidus phases [2], [3]. Generally, two major aspects are involved in gas–liquid flow characterization: one is the recognition of flow patterns [4], and the other is the establishment of quantitative correlation of flow parameters [5].

Accurate and effective identification of flow patterns is the basis for measurement and control of most other parameters in a gas–liquid system. The methods for discerning gas–liquid two-phase flow patterns have been investigated extensively. Among them, flow pattern maps, flow visualization and soft sensing are receiving much popularity. Constructing a flow pattern map is a classical method in recognition of flow patterns. Due to the boundary of flow pattern transition, flow patterns are determined by the determination of corresponding specific flow parameters according to the coordinates of the map [6]–[8]. A considerable number of widely

adaptable flow pattern maps are established, for instance, the Baker-Scott and the Hewitt maps which are appropriate for horizontal and vertical upward gas–liquid pipe flows [9]. Flow visualization techniques extract qualitative and quantitative information from fluid flow field by making it visible, and have solved numerous gas–liquid flow pattern identification problems [10]. Soft sensing provides a feasible alternative to impractical physical measurement issues, using parameters available from other sources of measurements to calculate the estimate of the quantity of interest. With the rapid development of computer and information processing technology, identification of gas–liquid flow patterns based on soft sensing becomes a useful and widely adopted tool in the field of multiphase flow measurement [11].

Normally, signals acquired for gas–liquid flow analysis are weak, so the differences between each flow pattern are hard to be distinguished. In this study, we proposed to utilize the fluid oscillation induced by a bluff body to strengthen the signals [12], [13]. Moreover, gas–liquid flow is known as a typical kind of complex, sensitive and nonlinear system whose behaviors are essentially difficult to be characterized
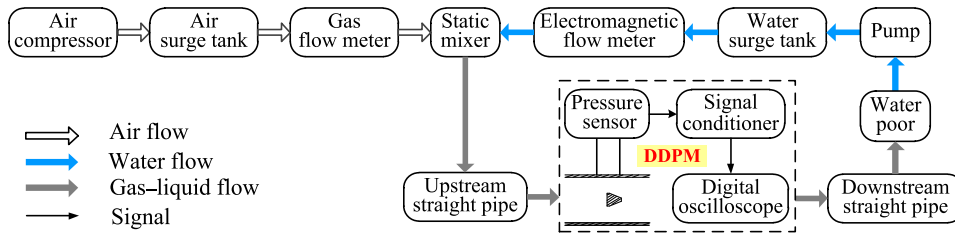
FIGURE 1. Schematic diagram of the experimental setups.

quantitatively. We introduced the correlation dimension as a means of analyzing fluid oscillation. As one of the fractal methods, the correlation dimension is quite sensitive to the unevenness of attractors in a system, and describes the internal structure and characteristic quantitatively. More specifically, it is capable of indicating the number of control systems and the degree of freedom of system dynamics, and it can also quantify the complexity of a system [14]. Correlation dimension has been successfully applied to processing signals in earthquake prediction and fault diagnosis [15], [16], providing a convincing nonlinear tool for seemingly disorganized, scattered and fragmented problems. Gas–liquid two-phase flow is nonlinear and dynamic-dissipated whose dynamic properties are surely better displayed by correlation dimension. It is viable to apply the correlation dimension to gas–liquid flow characterization.

The artificial neural network (ANN) is a kind of intelligent information processing systems which imitate the structure and function of human brains. It has been proved to be a useful tool for studying difficult processes that can not be described with simple mathematical models. Many investigations show that ANN is suitable for gas–liquid flow characterization, especially for flow pattern identification. For example, Fang *et al.* [17] resolved two-component fluid flow regimes adopting back-propagation networks trained on a series of simulated data of a capacitance tomography sensor. Yan *et al.* [18] identified gas–liquid flow patterns through ANN-based pressure fluctuation analysis. Hernandez *et al.* [19] achieved fast classification of gas–liquid flow regimes based on conductivity signals with ANN. Rosa *et al.* [20] compared the performance of different ANNs for flow pattern recognition in upward vertical air–water flows. Ghosh *et al.* [21] predicted flow regimes using conductivity probe signals and ANN in counter-current gas–liquid flows.

To achieve the purpose mentioned above, this study was arranged as follows. First, vortex-induced pressure fluctuation signals were acquired experimentally. Correlation dimension was calculated based on the signals, and parameters of interest that were most representative of the gas–liquid two-phase flow behaviors were identified using ANN. The chosen parameters were combined and used as the coordinates to construct a new flow pattern map. Ultimately, quantitative relationship between the parameters and the correlation dimension was established.
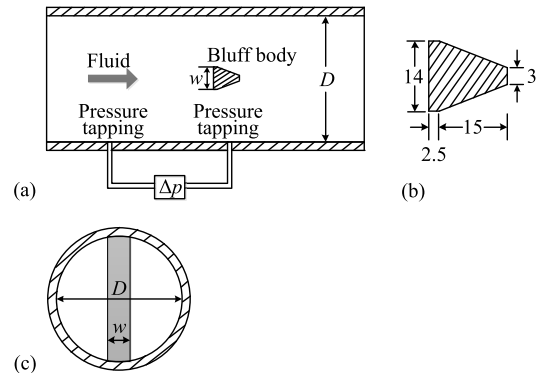

FIGURE 2. Sectional view of the bluff body: (a) Overall structure; (b) Dimensions of the bluff body (unit: mm); (c) Side view.

II. EXPERIMENTS

The gas–liquid two-phase flow experiments, adopting air and water as working fluids, were carried out in a horizontal loop at the ambient temperature and atmospheric pressure, as shown in Fig. 1. The air sucked by the compressor or the water pumped from the pool was first pressed into a surge tank to make smooth before its flow rate was measured, respectively. The volumetric air flow rate q_{vg} was obtained by the combined use of a vortex flowmeter (1.0% accuracy) and two rotameters (1.5% accuracy) in view of range abilities, while the volumetric water flow rate q_{vl} was acquired using an electromagnetic flowmeter (0.5% accuracy). In the experiments the volumetric flow rates of air and water were varied within 0.3–130 $m^3 \cdot h^{-1}$ and within 0.5–18.5 $m^3 \cdot h^{-1}$. Simultaneously, the temperature and pressure of the air and water adjacent to the flowmeters and at the test section were also recorded to calculate the void fractions and the local superficial velocities.

After their flow rates were measured, the air and water were well mixed through a static mixer and flowed over a prismatic bluff body that was mounted in the test pipe perpendicular to the fluid flow direction. The inner diameter D of the test pipe was 50 mm. The cross section of the bluff body was a truncated isosceles triangle with a front face width $w = 14$ mm embedded in the pipe, as plotted in Fig. 2. So the blockage ratio of the bluff body to the test section was $b = w/D = 0.28$, which could generate regular and intensive vortex shedding in the bluff body wake. Herein the vortex-induced pressure fluctuation over the bluff body were detected by the

Duct-wall Differential Pressure Method (DDPM) [22], [23] using a piezoresistive sensor with a response time 1.0 ms. The two pressure tappings were located $1.0D$ upstream and $0.2D$ downstream of the front face of the bluff body, where the signals with better quality, stability and intensity could be acquired. The pressure signals were collected by a 500-MHz-bandwidth digital oscilloscope. The sampling rate of 1 kHz was employed throughout the experiments and 10^4 points were included in each data set.

The upstream and downstream straight pipes connecting the bluff body were $70D$ and $50D$ long, which ensured the flow patterns fully developed in the test section. During each group of experiments the water flow rate was kept constant, whereas the air was added in incremental amounts step by step. When the maximum air flow rate reached, the water flow rate was shifted to a new value, and then the air flow rate was repeated to increase from 0 gradually. Correspondingly, the flow pattern in the test section was transformed from a single-phase flow to bubble, bubble/plug transitional, plug, slug, and annular flow. The flow patterns were observed manually from a section of transparent pipe installed in front of the bluff body.

The local volumetric air flow rate at the test section was derived from the perfect gas equation:

$$q_{\mathrm{vg,test}} = \frac{q_{\mathrm{vg}}(t_{\mathrm{test}} + 273.15)(p_{\mathrm{g}} + p_{\mathrm{atm}})}{(t_{\mathrm{g}} + 273.15)(p_{\mathrm{test}} + p_{\mathrm{atm}})} \quad (1)$$

where q_{vg}, t_{g}, and p_{g} were the volumetric flow rate, temperature, and pressure of the single-phase air measured in front of the static mixer, t_{test} and p_{test} were the temperature and pressure of the gas–liquid mixture measured at the test section, and p_{atm} represents the atmospheric pressure.

The experiments were conducted at ambient temperature and atmospheric pressure; therefore, the volumetric water flow rate kept invariant due to its negligible compressibility. Hence the flow-rate based void fraction was calculated by

$$\beta = \frac{q_{\mathrm{vg,test}}}{q_{\mathrm{vg,test}} + q_{\mathrm{vl}}} \quad (2)$$

where q_{vl} was the volumetric water flow rate measured in front of the static mixer.

The superficial velocities of the gas and liquid phase were computed from

$$u_{\mathrm{g}} = \frac{4q_{\mathrm{vg,test}}}{\pi D^2} \quad (3)$$

$$u_{\mathrm{l}} = \frac{4q_{\mathrm{vl}}}{\pi D^2} \quad (4)$$

III. CALCULATION OF CORRELATION DIMENSION

The method proposed by Grassberger and Procaccia [24], was adopted to calculate the correlation dimension D_2 basing on reconstruction of phase space, with embedding dimension m and time delay τ. Since the computation cost of D_2 increased markedly with the increase of m, three thousand data points were used in this study to compromise between the appropriate amount for obtaining D_2 and the computation efficiency.

A. SELECTION OF PARAMETERS

The embedding dimension m and the time delay τ directly affected the reliability of quantitative analysis of the fractal characteristics, and it was assumed that the choice of m and τ were inseparable and complementary to each other.

Generally, m should satisfy the condition: $m \geq 2d + 1$, where d was the true dimension of the space in which the attractor of the original state space was located [25]. If m was small, it would produce many false crosses so that the attractor of the system could not be depicted correctly; otherwise, if m was too large, the noise of the time series was embedded in the phase space and the characteristics of the original system would be masked by noise. The embedding dimension m was determined when the correlation dimension became stable with the increment of m.

On the other hand, if τ was too small, two points in the phase space would be very close to each other and the trajectory might squeeze to the same position in the phase space, which would lead to the difficulties in revealing the internal information and miscellaneous errors. If τ was too large, two points in the phase space would lose association resulting in dramatic changes of dynamic shape and the simple geometric objects would become more complex, preventing the acquisition of good reflection of characteristics and inherent law of the system. In this study, the C-C method proposed by Kim with good anti-noise ability [26], [27], was used to calculate the time delay τ.

B. RECONSTRUCTION OF PHASE SPACE

The given time series of a dynamic system $x_k = x(k \Delta t)$, $(k = 1, 2, 3, \ldots, N)$ was embedded into a m-dimensional space to fully expose the information contained in the time series. For this phase space, it was converted into a set as follows:

$$X_n(m, \tau) = \{x_n, x_{n+k}, x_{n+2k}, \ldots, x_{n+(m-1)k}\} \quad (5)$$

where $\tau = k \Delta t$ was the time delay, Δt was the sampling interval, X_n was the N vector in m-dimensional space, $n = 1, 2, 3, \ldots, M$, and $M = N - (m - 1)\tau$ was the total number of vectors in reconstructed m-dimensional phase space.

So the reconstructed phase space was defined as

$$X = [X_1(m, \tau), X_2(m, \tau), \cdots, X_M(m, \tau)]^{\mathrm{T}} \quad (6)$$

If k was equal to 2, then X could be expressed as [28]

$$X = \begin{bmatrix} x_1 & x_3 & \ldots & x_{2m-1} \\ x_2 & x_4 & \ldots & x_{2m} \\ x_3 & x_5 & \ldots & x_{2m+1} \\ \ldots & \ldots & \ldots & \ldots \\ x_{N-2m+2} & x_{N-2m+4} & \ldots & x_N \end{bmatrix} \quad (7)$$

We reconstructed the original dynamical rules through the point trajectory which described the evolution from an initial state and represent the history of the system [29]. In this paper, we employed the fractal feature, the correlation dimension, to describe the complexity of the system.

C. CALCULATION PROCEDURE

First we calculated the distance between all the vectors in the phase space. We defined the phase point X_i, which was chosen arbitrarily from the M data points, as the reference phase point and calculated the spatial distance d_{ij} between X_i and the other $M - 1$ phase points:

$$d_{ij} = \left\| X_i - X_j \right\| \tag{8}$$

where X_i and X_j were the two points in the phase space reconstruction.

After calculating all the points, the correlation integral could be obtained as

$$C(r) = \frac{2}{M(M-1)} \sum \theta(r - d_{ij}), r > 0 \tag{9}$$

where $r > 0$, and $1 \leq i \leq j \leq M$.

$C(r)$ represented the percentage of the number of point pairs in the phase space whose radius was smaller than r, and $\theta(x)$ was the Heaviside function, which was defined as

$$\theta(x) = \begin{cases} 0, & x < 0 \\ 1, & x \geq 0 \end{cases} \tag{10}$$

Therefore, the correlation dimension D_2 was calculated by the correlation integral $C(r)$ and the radius r with

$$D_2 = \frac{\mathrm{d}\ln C(r)}{\mathrm{d}\ln r} \tag{11}$$

D_2 was regarded as the slope of the $\ln C(r)$-$\ln r$ line segments when r was in a relatively small value and the correlation of $\ln C(r)$ with $\ln r$ was indicated approximately straight. With a growing m, D_2 increased and became saturated gradually [17].

IV. RESULTS AND DISCUSSION

A. RAW PRESSURE FLUCTUATIONS ACROSS THE BLUFF BODY

Typical fluctuating pressure signals across the bluff body of each of the flow patterns observed in the experiments are given in Fig. 3. As for the bubble flow, Kármán vortex street could still be maintained in despite of a dispersion of gas within the liquid continuum, and the fairly regular pressure fluctuation as shown in Fig.3a corresponded to the fluid oscillation induced by the regular vortex shedding. In the other four flow patterns, however, pressure fluctuations exhibited pronounced diversity in frequency and amplitude variation. Regular vortex shedding disappeared. The pressure fluctuations obtained under other experimental conditions are similar to those in Fig.3 within an identical flow pattern. The differences in the raw signals of various flow patterns provide a feasibility to identify gas–liquid flow patterns based on the pressure fluctuations across a bluff body. However, it is hardly possible to discern flow patterns quantitatively from the time series of the signals, so advanced methods of processing and analyzing the pressure fluctuations are needed.
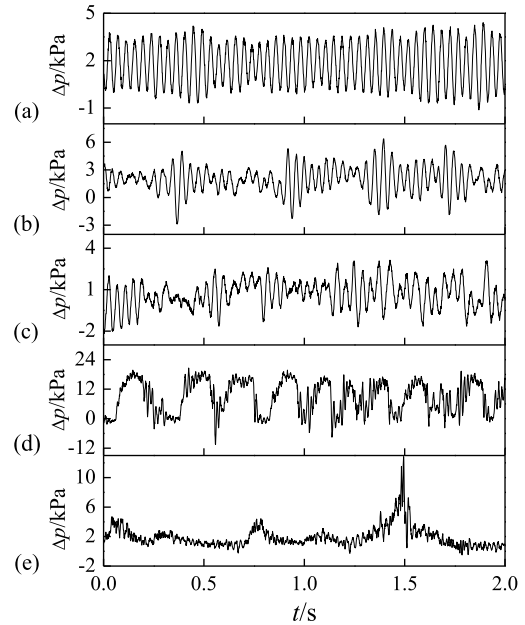
FIGURE 3. Vortex-induced pressure fluctuations: (a) Bubble flow; (b) Bubble/plug transitional flow; (c) Plug flow; (d) Slug flow; (e) Annular flow.
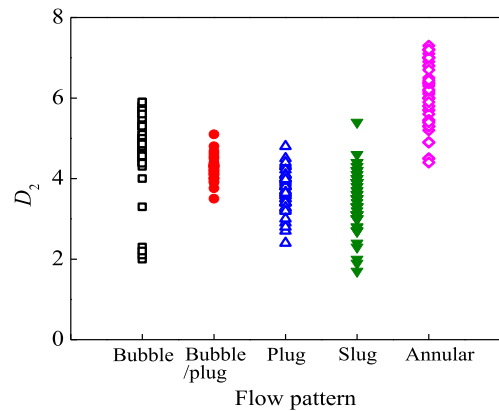

FIGURE 4. Distribution of the correlation dimensions in different flow patterns.

B. CONSTRUCTION OF THE CORRELATION DIMENSION BASED FLOW PATTERN MAP

As given in Fig. 4, the correlation dimension of each flow pattern was calculated in accordance to the steps described in Section 3. For all the flow patterns, the values of the correlation dimensions distributed widely in general, which revealed the complex dynamic essence of the gas–liquid flow systems due to the intricate and random motion of dispersed phase. In addition, the existence of the bluff body and the vortex shedding under certain conditions made the flow structure more complicated.

The correlation dimensions of the bubble and the annular flows were comparatively larger than those of the other flow patterns. When the fraction of the dispersed phase was below a certain value, its existence had merely limited influence on the generation of the vortex shedding behind the bluff body
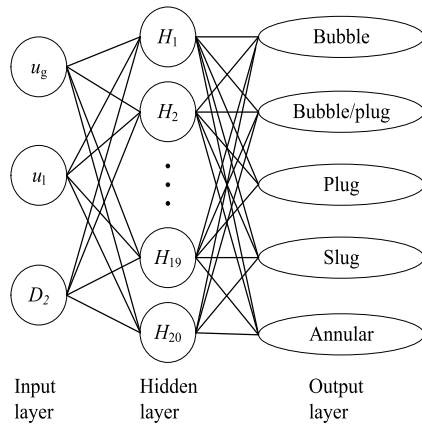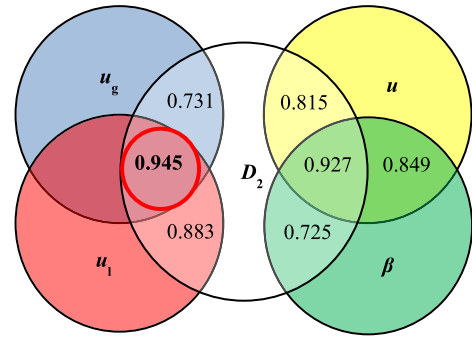
FIGURE 5. Structure of the artificial neural network using u_l, u_g and D_2 as inputs.

FIGURE 6. Partial flow pattern recognition accuracies of the artificial neural network using different combinations of inputs.

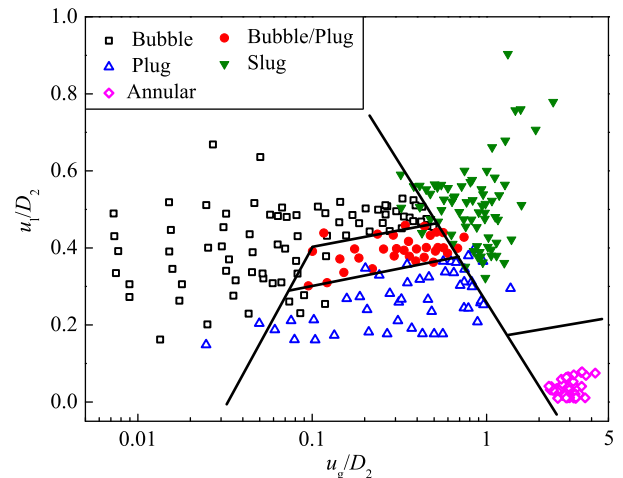**FIGURE 7.** The constructed gas–liquid two-phase flow pattern map.

in the continuous phase. While with the increase of the void fraction, the dispersed phase suppressed the yielding of vortex shedding, so the dynamic characteristics of the gas–liquid system became relatively simple and the corresponding correlation dimension decreased. As for the bubble and the annular flows, the content of the dispersed phase were comparatively low; therefore, their correlation dimensions increased.

Different flow patterns had different correlation dimension distribution. It is possible to utilize the correlation dimension extracted from the vortex-induced pressure fluctuations as a rational characteristic indicator for gas–liquid two-phase flow pattern recognition. We introduced the correlation dimension into the construction of a novel flow pattern map. The back propagation (BP) network, one of the most widely used ANNs, was employed to simplify the construction process, helping select the appropriate variables from a large quantity of flow parameters to form the horizontal and vertical ordinates on the map. The adopted feed-forward topology, consisting of one input layer of 2 or 3 input neurons, one hidden layer of 20 sigmoid neurons and one output layer of 5 neurons, is presented in Fig. 5. The BP network was trained by the scaled conjugate gradient back propagation algorithm, and its performance was evaluated using the cross-entropy algorithm whose consecutive decrease in six iterations was taken as the termination criterion of the training process [30].

Flow parameters, such as gas superficial velocity u_g, liquid superficial velocity u_l, total superficial velocity u, void fraction β and correlation dimension D_2, constituting a number of two-element or three-element combinations, were fed into the ANN as the input layer. About two-thirds of the experimental data was randomly selected for training, whereas the remaining was used for testing. For each combination of inputs, the ANN was trained ten times independently while the model accuracy was the average value of the ten runs. The results of partial combinations are shown in Fig. 6. It is found that the u_g, u_l and D_2 combination as the ANN's input achieved the best accuracy for flow pattern identification, and the recognition accuracies of the other combinations were basically in the range of 0.7–0.8 or less. Therefore,

u_g and u_l are determined as the most appropriate variables to be involved in the correlation dimension based flow pattern map.

By trial and error, various forms of u_g, u_l and D_2 combination were used to construct flow pattern map that can distinguish gas–liquid two-phase flow patterns with clear boundaries and reasonable accuracies. Ultimately, we adopted u_g/D_2 as the horizontal coordinate and u_l/D_2 as the vertical coordinate to shape the new flow pattern map, as demonstrated in Fig. 7. The distinction of different flow patterns is considerably acceptable in many industrial applications, except for the mixing of the bubble/plug transition flow. Due to the absence of objective criterion during the transition of flow patterns, some mixed and overlapping problems on the boundary between adjacent flow patterns were inevitable. Moreover, we also plotted the results on some current existing flow pattern maps, such as the Bake's map, it shows that the distinction performance of the proposed method is superior.

C. RELATIONSHIP BETWEEN THE CORRELATION DIMENSION AND THE SUPERFICIAL VELOCITIES
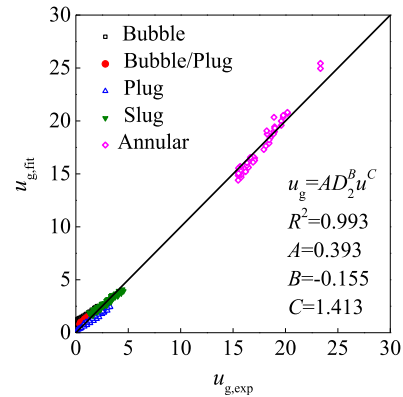Fig. 7 indicates that the transition of gas–liquid flow patterns was strongly correlated with the superficial velocities and the correlation dimension. In this section, we further

(a)

(b)

(c)

(d)
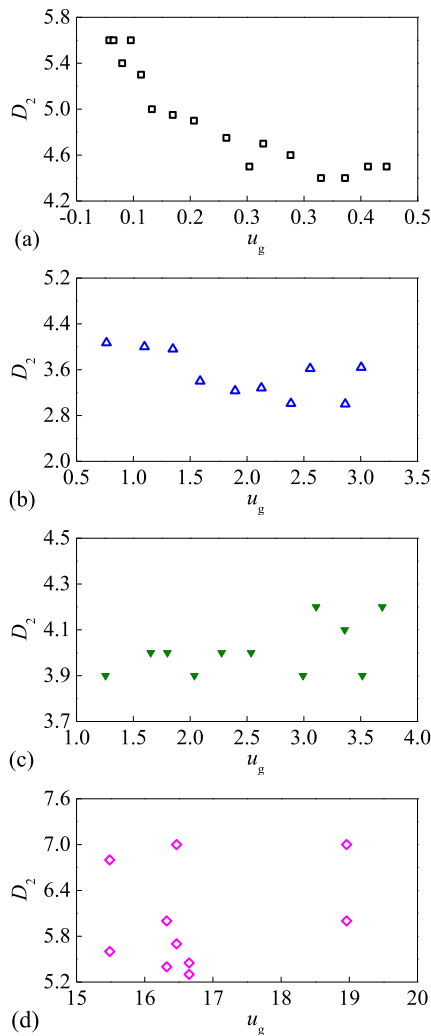
FIGURE 8. Correlation dimension versus gas superficial velocity: (a) Bubble flow at u_{l0} = 2.19m/s; (b) Plug flow at u_{l0} = 1.12 m/s; (c) Slug flow at u_{l0} = 2.64 m/s; (d) Annular flow at u_{l0} = 0.28 m/s.

$$u_g = AD_2^B u^C$$
$$R^2 = 0.993$$
$$A = 0.393$$
$$B = -0.155$$
$$C = 1.413$$

FIGURE 9. The fitting for all flow patterns with the same set of coefficients.

examined the relationship between these variables. Since the flow patterns varied with both the gas superficial velocity and the liquid superficial velocity, the following discussion only accounted for the results at a fixed liquid superficial velocity to simplify the analysis. The tendency of the correlation dimension versus the gas superficial velocity is presented in Fig. 8, and the initial liquid superficial velocity u_{l0} was maintained invariant in its each subfigure. It is noted that the cases for the bubble/plug transitional flow are not given because this flow pattern did not appear adequately during the experiments and its tendency exhibited no obvious regularity.

Fig. 8a shows the correlation dimension of bubble flows at initial liquid superficial velocity u_{l0} = 2.19 m/s. The correlation dimension decreased gradually with the increase of the gas superficial velocities, suggesting that the complexity of the gas–liquid bluff body wake was lowered by the introduction of more amount of gas. Fig. 8b and Fig. 8c respectively shows the correlation dimension of the plug and the slug flows, which both fluctuated at a relatively small

value around 4.0 compared to those of the bubble flows. As given in Fig. 8d, the correlation dimension of annular flows exhibited more marked fluctuation with the increase of gas superficial velocities, and its average value was about 6.0, much bigger than those of the other three flow patterns. It reveals that the strong separate flow of gas and liquid phase in annular flows made the bluff body wake become supremely complex.

Since we have found that there was close relation between the correlation dimension and the superficial velocities, a quantitative relationship between these parameters can be supposedly established for the entire regime with respect to each pattern. After trials, the multivariate nonlinear fitting, $u_g = AD_2^B u^C$, was able to produce an acceptably accurate universal correlation for all flow pattern as presented in Fig. 9, while possessing justifiable physical meaning. On the left of this formula was the gas superficial velocity u_g, and the right side was the product of a constant A, the correlation dimension D_2 to the Bth power and the total superficial velocity u to the Cth power. The addition of gas phase within the model resulted in certain change in the dynamic complexity of the system, which was reflected by the correlation dimension, with the exponent B for the degree of the influence. Since the changing complexity was imposed on the entire system, also included in the product was the total superficial velocity, whose influence was reflected by the exponent C. The constant A was served as an overall adjusting coefficient.

The data of all five flow patterns could be correlated by the formula, producing the following results with the coefficient of determination R^2 = 0.993. However, for $u_g < 5$ m/s, the fitting contained considerable local inaccuracies which indicated the inadequate matching with the bubble flows. For this reason, more accurate correlations were proposed for each flow pattern which took the same form but different values of the coefficient. The coefficient of determination R^2 for each pattern suggested a fairly good fit, as shown in Fig. 10a–e. Then, compiling the five pattern-specific fittings into one graph resulted in a fitting with R^2 approaching to 1 closely, that is to say, adopting different fittings for different
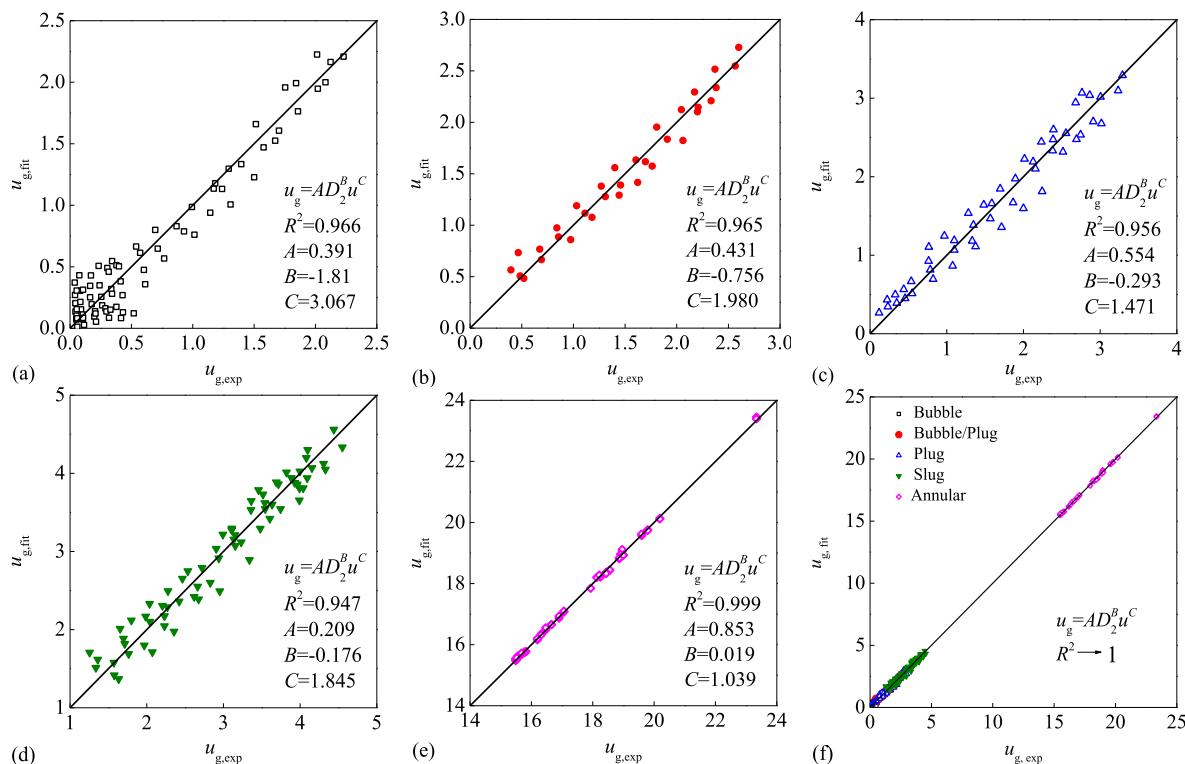
FIGURE 10. The fitting for each specific flow pattern: (a) Bubble flow; (b) Bubble/plug transitional flow; (c) Plug flow; (d) Slug flow; (e) Annular flow; (f) All flow patterns with each set of coefficients.

flow patterns achieved better results, as shown in Fig. 10f. It is obvious that compared with the previous one, the fitting for the bubble flow did not contain noticeable inaccuracy. In summary, a more precise quantitative correlation between the gas superficial velocity and correlation dimension was established. As a result, when one of the three superficial velocities is given, we can calculate the other two with the aid of the correlation dimension. Furthermore, the volumetric flow rate of gas or liquid phase can be obtained as well as the void fraction.

V. CONCLUSIONS

The correlation dimension extracted from the fluctuating pressure induced by a bluff body was applied to characterize gas–liquid two-phase flow behaviors in this study. With the help of a trained ANN for selecting appropriate coordinate combinations of flow parameters and the correlation dimension, a new gas–liquid flow pattern map was constructed, which was able to distinguish between the bubble, bubble/ plug transitional, plug, slug, and annular flows with quite reasonable accuracy. Furthermore, quantitative relationships between the correlation dimension and the superficial velocities were established by the universal and the pattern-specific fittings with the coefficients of determination R^2 close to 1. Inevitably, the establishment of this method is rather subjective and may lack universality, so more tests are needed to be conducted to evaluate and extend its applicability under other experimental conditions.

REFERENCES

[1] J. E. Juliá, Y. Liu, S. Paranjape, and M. Ishii, "Upward vertical two-phase flow local flow regime identification using neural network techniques," *Nucl. Eng. Des.*, vol. 238, no. 1, pp. 156–169, Jan. 2008.

[2] C. Tan, F. Dong, and M. Wu, "Identification of gas/liquid two-phase flow regime through ERT-based measurement and feature extraction," *Flow Meas. Instrum.*, vol. 18, nos. 5–6, pp. 255–261, Oct. 2007.

[3] J. Zhang, K. Xu, S. Dong, Z. Liu, Q. Hou, and Z. Fang, "Mathematical model of time difference for coriolis flow sensor output signals under gas-liquid two-phase flow," *Measurement*, vol. 95, pp. 345–354, Jan. 2017.

[4] A. Mahvash and A. Ross, "Two-phase flow pattern identification using continuous hidden Markov model," *Int. J. Multiphase Flow*, vol. 34, no. 3, pp. 303–311, Mar. 2008.

[5] S. Haase, "Characterisation of gas-liquid two-phase flow in minichannels with co-flowing fluid injection inside the channel, part II: Gas bubble and liquid slug lengths, film thickness, and void fraction within Taylor flow," *Int. J. Multiphase Flow*, vol. 88, pp. 251–269, Jan. 2016.

[6] Z. Sun, S. Shao, and H. Gong, "Gas-liquid flow pattern recognition based on wavelet packet energy entropy of vortex-induced pressure fluctuation," *Meas. Sci. Rev.*, vol. 13, no. 2, pp. 83–88, May 2013.

[7] Z. Sun and H. Gong, "Energy of intrinsic mode function for gas-liquid flow pattern identification," *Metrol. Meas. Syst.*, vol. 19, no. 4, pp. 759–766, May 2012.

[8] Z. Sun, Y. Chen, and H. Gong, "Classification of gas-liquid flow patterns by the norm entropy of wavelet decomposed pressure fluctuations across a bluff body," *Meas. Sci. Technol.*, vol. 23, no. 12, p. 125301, Dec. 2012.

[9] Y. Xu, P. Yu, Z. Zhu, Y. Chao, and T. Zhang, "Over-reading modeling of the ultrasonic flow meter in wet gas measurement," *Measurement*, vol. 98, pp. 17–24, Feb. 2017.

[10] R. Banasiak *et al.*, "Study on two-phase flow regime visualization and identification using 3D electrical capacitance tomography and fuzzy-logic classification," *Int. J. Multiphase Flow*, vol. 58, pp. 1–14, Jan. 2014.

[11] G. H. Roshani, E. Nazemi, and M. M. Roshani, "Usage of two transmitted detectors with optimized orientation in order to three phase flow metering," *Measurement*, vol. 100, pp. 122–130, Mar. 2007.

[12] S. Li, T. Zhou, Z. Sun, and Z. Dong, "External forced convection from circular cylinders with surface protrusions," *Int. J. Heat Mass Transf.*, vol. 99, pp. 20–30, Aug. 2016.

[13] S. Li and Z. Sun, "Harvesting vortex energy in the cylinder wake with a pivoting vane," *Energy*, vol. 88, pp. 783–792, Aug. 2015.

[14] W. Zhang, S. Tan, P. Gao, Z. Wang, L. Zhang, and H. Zhang, "Non-linear time series analysis on flow instability of natural circulation under rolling motion condition," *Ann. Nucl. Energy*, vol. 65, pp. 1–9, Mar. 2014.

[15] A. Rolo-Naranjo and M.-E. Montesino-Otero, "A method for the correlation dimension estimation for on-line condition monitoring of large rotating machinery," *Mech. Syst. Signal Process.*, vol. 19, no. 5, pp. 939–954, Sep. 2005.

[16] L. Lian, W. Song, J. Ma, and L. Telesca, "Correlation dimension of collective versus individual pedestrian movement patterns in crowd-quakes: A case-study," *Phys. A, Statist. Mech. Appl.*, vol. 452, pp. 113–119, Jun. 2016.

[17] L. Fang, Y. Liang, Q. Lu, X. Li, R. Liu, and X. Wang, "Flow noise characterization of gas–liquid two-phase flow based on acoustic emission," *Meas.*, vol. 46, no. 10, pp. 3887–3897, Dec. 2013.

[18] H. Yan, Y. Liu, and C. Liu, "Identification of flow regimes using back-propagation networks trained on simulated data based on a capacitance tomography sensor," *Meas. Sci. Technol.*, vol. 15, no. 2, pp. 432–436, Feb. 2004.

[19] L. Hernández, J. E. Juliá, S. Paranjape, and M. Ishii, "Fast classification of two-phase flow regimes based on conductivity signals and artificial neural networks," *Meas. Sci. Technol.*, vol. 17, no. 6, pp. 1511–1521, Jun. 2006.

[20] E. S. Rosa, R. M. Salgado, T. Ohishi, and N. Mastelari, "Performance comparison of artificial neural networks and expert systems applied to flow pattern identification in vertical ascendant gas-liquid flows," *Int. J. Multiphase Flow*, vol. 36, no. 9, pp. 738–754, Sep. 2010.

[21] S. Ghosh, D. K. Pratihar, B. Maiti, and P. K. Das, "Identification of flow regimes using conductivity probe signals and neural networks for counter-current gas–liquid two-phase flow," *Chem. Eng. Sci.*, vol. 84, no. 52, pp. 417–436, Dec. 2012.

[22] Z. Sun, H. Zhang, and J. Zhou, "Investigation of the pressure probe properties as the sensor in the vortex flowmeter," *Sens. Actuators A, Phys.*, vol. 136, no. 2, pp. 646–655, May 2007.

[23] Z. Sun, H. Zhang, and J. Zhou, "Evaluation of uncertainty in a vortex flowmeter measurement," *Measurement*, vol. 41, no. 4, pp. 349–356, May 2008.

[24] P. Grassberger and I. Procaccia, "Dimensions and entropies of strange attractors from a fluctuating dynamics approach," *Phys. D, Nonlinear Phenom.*, vol. 13, nos. 1–2, pp. 34–54, Aug. 1984.

[25] F. Takens, "Detecting strange attractors in turbulence," in *Dynamical Systems and Turbulence, Warwick* (Lecture Notes in Mathematics), vol. 898. Berlin, Germany: Springer, Aug. 1981, pp. 366–381.

[26] H. S. Kim, R. Eykholt, and J. D. Salas, "Nonlinear dynamics, delay times, and embedding windows," *Phys. D, Nonlinear Phenom.*, vol. 127, nos. 1–2, pp. 48–60, Mar. 1999.

[27] Z. Gao and N. Jin, "Flow-pattern identification and nonlinear dynamics of gas-liquid two-phase flow in complex networks," *Phys. Rev. E, Stat. Phys. Plasmas Fluids Relat. Interdiscip. Top.*, vol. 79, no. 2, p. 066303, Jun. 2009.

[28] X. Tian, Y. Li, and X. Li, "Hybrid algorithm for traction transformer differential protection based on intrinsic mode function energy entropy and correlation dimension," *IET Generat. Transm. Distrib.*, vol. 8, no. 7, pp. 1274–1283, Jul. 2014.

[29] J. Y. Lee, N. S. Kim, and M. Ishii, "Flow regime identification using chaotic characteristics of two-phase flow," *Nucl. Eng. Des.*, vol. 238, no. 4, pp. 945–957, Apr. 2008.

[30] T. Xie, S. M. Ghiaasiaan, and S. Karrila, "Flow regime identification in gas/liquid/pulp fiber slurry flows based on pressure fluctuations using artificial neural networks," *Ind. Eng. Chem. Res.*, vol. 42, no. 26, pp. 7017–7024, Nov. 2003.

SISHI HUANG was born in Changsha, China, in 1993. She received the B.S. degree from Central South University, China, in 2010, where she is currently pursuing the M.S. degree with the School of Energy Science and Engineering. Her research area is analysis of multiphase flow field.

JIAWEN YIN was born in Shaanxi, China, in 1997. She is currently pursuing the B.S. degree with the School of Energy Science and Engineering, Central South University. Her research interest is multiphase flow.

ZHIQIANG SUN received the Ph.D. degree from Zhejiang University, China. From 2011 to 2012, he was a Visiting Scholar with Duke University, NC, USA. He is currently a Professor with the School of Energy Science and Engineering, Central South University, China. He is also the Vice Dean of the school and the Director of the Institute of Automation and Informatization for Energy Systems. He is the author or co-author of four books and has authored more than 80 peer-reviewed academic papers. His major research area is measurement techniques for multiphase flows, and design and optimization of thermofluids systems. He received a grant from the New Century 121 Talents and Young Talents of Hunan Province.

SAIWEI LI received the B.S. and M.S. degrees from Central South University in 2012 and 2015, respectively. He is currently pursuing the Ph.D. degree with the School of Energy Science and Engineering, Central South University, China. His major research area is the fundamental and application of multiphase flows, and the design and optimization of thermofluids systems. He has authored two peer-reviewed academic papers.

TIAN ZHOU was born in Changsha, China, in 1984. He received the B.S. degree in automation engineering from Central South University in 2006, the M.S. degree in microsystem integration technology from Chalmers in 2009, and the Ph.D. degree in thermal engineering from Central South University in 2014. He is currently a Lecturer with the School of Energy Science and Engineering, Central South University. His research interests include multiphase flow and thermal-physical property measurement.

• • •